

Lake Heat Flux Analyzer

user manual

by Richard Iestyn Woolway

Version 1.0, October 6, 2014

Contributors

We would like to thank the Global Lake Ecological Observatory Network (GLEON) and the Networking Lake Observatories in Europe (NETLAKE) for their support in developing the Lake Heat Flux Analyzer program. The material used in this program is due to the combined effort of the following individuals:

R. Iestyn Woolway <riwoolway@gmail.com>, *Centre for Ecology*

& Hydrology, Lancaster, United Kingdom

Ian D. Jones <ianj@ceh.ac.uk>, *Centre for Ecology & Hydrology,*

Lancaster, United Kingdom

David P. Hamilton <davidh@waikato.ac.nz>, *Environmental Re-*

search Institute, University of Waikato, New Zealand

Stephen C. Maberly <scm@ceh.ac.uk>, *Centre for Ecology and*

Hydrology, Lancaster, United Kingdom

Kohji Muraoka <km112@waikato.ac.nz>, *Environmental Research*

Institute, University of Waikato, New Zealand

Jordan S. Read <jread@usgs.gov>, *U.S. Geological Survey Cen-*

ter for Integrated Data Analytics, Wisconsin, USA

Robyn L. Smyth <rsmyth@bard.edu>, *Center for Environmental
Policy, Bard College, New York, USA*

Luke A. Winslow lawinslow@gmail.com, *Center for Limnology,
University of Wisconsin-Madison, USA*

Lake Heat Flux Analyzer is in active development, and we encourage individuals who would like to contribute to the code to contact the lead author.

Preface

Lake Heat Flux Analyzer is a numerical code for calculating the surface energy fluxes in lakes. The program was developed for the rapid analysis of high-frequency instrumented lake buoy data in support of the emerging field of aquatic sensor network science. The purpose of this user manual is to describe the physical parameterization and numerical implementation of the Lake Heat Flux Analyzer program. Scientific justification and evaluation of these parameterizations can be found in the referenced scientific papers. This manual is split into three chapters:

Chapter 1 includes a description of the basic structure of Lake Heat Flux Analyzer and how to format the input files.

Chapter 2 goes into the details of the operation of the program as well as introducing the online application.

Chapter 3 explains the various terms of the surface energy fluxes and how these fluxes are calculated within the Lake Heat Flux Analyzer program.

Source code for Lake Heat Flux Analyzer is available at
<https://github.com/GLEON/HeatFluxAnalyzer> and the online application
can be found at <http://heatfluxanalyzer.gleon.org/>.

Contents

1	Input file formats	1
1.1	Water temperature	2
1.2	Wind speed	2
1.3	Air temperature	2
1.4	Relative humidity	3
1.5	Short-wave radiation	3
1.6	Net long-wave radiation	3
1.7	Incoming long-wave radiation	4
1.8	Photosynthetically active radiation	4
1.9	Configuration file	5
1.10	Example input files	5
2	Program operation	10
3	Bulk parameterization of surface fluxes	15
3.1	Incident and reflected short-wave radiation	16
3.2	Long-wave radiation	17

3.3	Bulk algorithms for momentum, sensible and latent heat fluxes	23
3.4	Evaporation	41

Chapter 1

Input file formats

Full performance of Lake Heat Flux Analyzer requires various input files, including a water temperature file (extension .wtr), wind data (.wnd), short-wave radiation (.sw), relative humidity (.rh), air temperature (.airT) and configuration file (.hfx). The program can also accept net long-wave radiation data (.lwnet), incoming long-wave radiation data (.lw) and photosynthetically active radiation data (.par). Names must be shared among files and the required text file format is tab-delimited. A list of the input files required for individual outputs can be found in Woolway et al (2014). All the input files should be located in an identical folder with the user defined name (i.e. lake name).

1.1 Water temperature

The water temperature file is a tab-delimited file with a file extension of (.wtr). The file should contain one header which starts with ‘dateTime’, followed by the temperature measurements. Lake Heat Flux Analyzer also accepts .wtr file in the same format as Lake Analyzer (Read et al., 2011) where individual thermistor depths are provided. Lake Heat Flux Analyzer will only use the first temperature column, and assume this is the temperature of the lake surface; all of the other columns will be ignored. The data starts from date/time inputs, which should be formatted as [yyyy-mm-dd HH:MM].

1.2 Wind speed

The wind speed file is a tab-delimited file with a file extension of (.wnd). The file should contain one header which starts with ‘dateTime’, followed by the wind speed, ‘wnd’. The data starts from date/time inputs, which should be formatted as [yyyy-mm-dd HH:MM], and wind speed data in m s^{-1} should be described.

1.3 Air temperature

The air temperature file is a tab-delimited file with a file extension of (.airT). The file should contain one header which starts with ‘dateTime’, followed by

the air temperature ‘airT’. The data starts from date/time inputs, which should be formatted as [yyyy-mm-dd HH:MM], and air temperature data in °C should be described.

1.4 Relative humidity

The relative humidity file is a tab-delimited file with a file extension of (.rh). The file should contain one header which starts with ‘dateTime’, followed by the relative humidity ‘rh’. The data starts from date/time inputs, which should be formatted as [yyyy-mm-dd HH:MM], and relative humidity data in % should be described.

1.5 Short-wave radiation

The short-wave radiation file is a tab-delimited file with a file extension of (.sw). The file should contain one header which starts from ‘dateTime’, followed by the short-wave radiation ‘sw’. The data starts from date/time inputs, which should be formatted as [yyyy-mm-dd HH:MM], and short-wave radiation data in W m^{-2} should be described.

1.6 Net long-wave radiation

The net long-wave radiation file is a tab-delimited file with a file extension of (.lwnet). The file should contain one header which starts from ‘date-

Time’, followed by the net long-wave radiation ‘lwnet’. The data starts from date/time inputs, which should be formatted as [yyyy-mm-dd HH:MM], and net long-wave radiation data in W m^{-2} should be described.

1.7 Incoming long-wave radiation

The incoming long-wave radiation file is a tab-delimited file with a file extension of (.lw). The file should contain one header which starts from ‘dateTime’, followed by the incoming long-wave radiation ‘lw’. The data starts from date/time inputs, which should be formatted as [yyyy-mm-dd HH:MM], and incoming long-wave radiation data in W m^{-2} should be described.

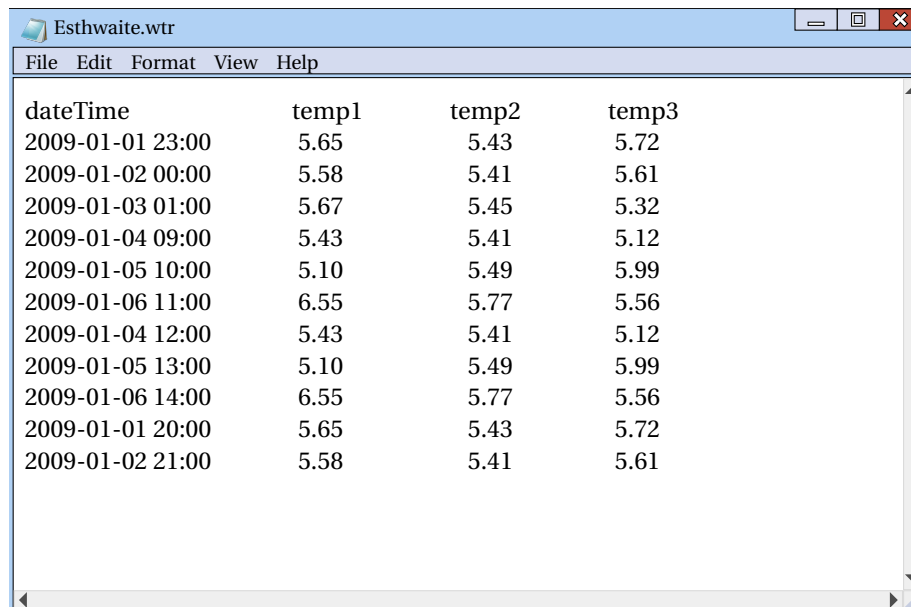
1.8 Photosynthetically active radiation

The photosynthetically active radiation file is a tab-delimited file with a file extension of (.par). The file should contain one header which starts from ‘dateTime’, followed by the photosynthetically active radiation ‘par’. The data starts from date/time inputs, which should be formatted as [yyyy-mm-dd HH:MM], and photosynthetically active radiation data in $\text{mmol m}^{-2} \text{s}^{-1}$ should be described.

1.9 Configuration file

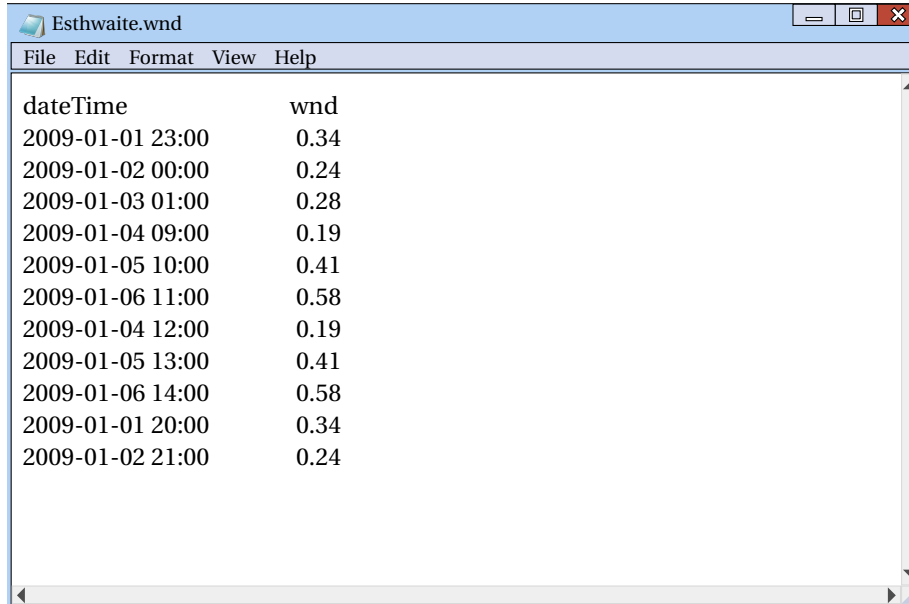
The configuration file manages the operation of Lake Heat Flux Analyzer with an extension of (.hfx). The configuration file is automatically created by Lake Heat Flux Analyzer through the configuration window. A list of input files required for each output is provided in Woolway et al., (2014).

1.10 Example input files



dateTime	temp1	temp2	temp3
2009-01-01 23:00	5.65	5.43	5.72
2009-01-02 00:00	5.58	5.41	5.61
2009-01-03 01:00	5.67	5.45	5.32
2009-01-04 09:00	5.43	5.41	5.12
2009-01-05 10:00	5.10	5.49	5.99
2009-01-06 11:00	6.55	5.77	5.56
2009-01-04 12:00	5.43	5.41	5.12
2009-01-05 13:00	5.10	5.49	5.99
2009-01-06 14:00	6.55	5.77	5.56
2009-01-01 20:00	5.65	5.43	5.72
2009-01-02 21:00	5.58	5.41	5.61

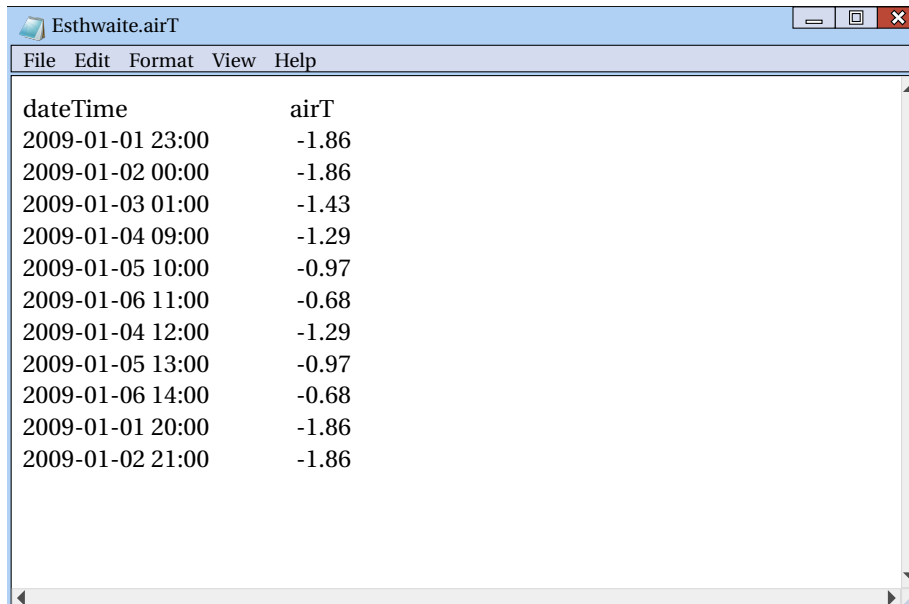
An example water temperature file used for Esthwaite Water.



The screenshot shows a text editor window titled "Esthwaite.wnd" with a menu bar (File, Edit, Format, View, Help). The window contains a table with two columns: "dateTime" and "wnd". The data is as follows:

dateTime	wnd
2009-01-01 23:00	0.34
2009-01-02 00:00	0.24
2009-01-03 01:00	0.28
2009-01-04 09:00	0.19
2009-01-05 10:00	0.41
2009-01-06 11:00	0.58
2009-01-04 12:00	0.19
2009-01-05 13:00	0.41
2009-01-06 14:00	0.58
2009-01-01 20:00	0.34
2009-01-02 21:00	0.24

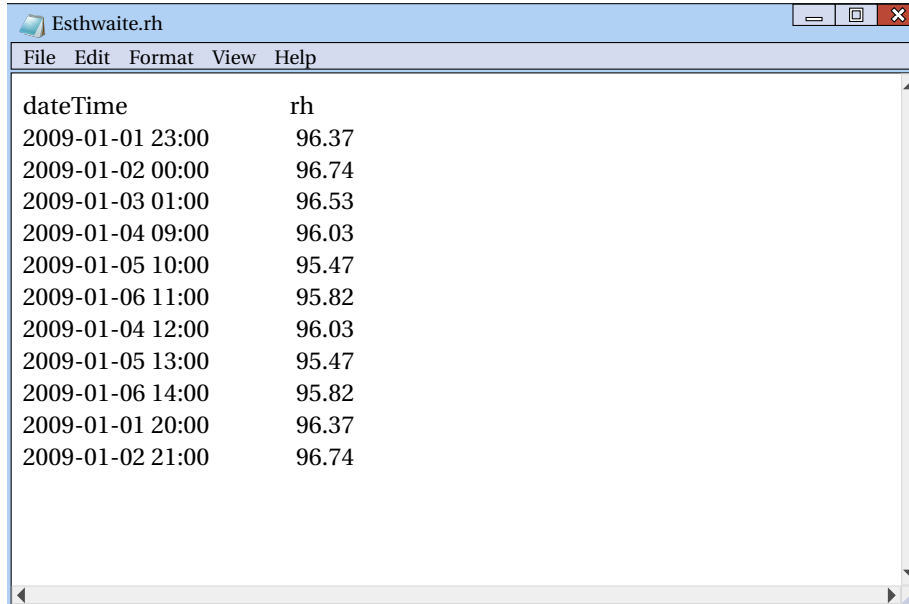
An example wind speed file used for Esthwaite Water.



The screenshot shows a text editor window titled "Esthwaite.airT" with a menu bar (File, Edit, Format, View, Help). The window contains a table with two columns: "dateTime" and "airT". The data is as follows:

dateTime	airT
2009-01-01 23:00	-1.86
2009-01-02 00:00	-1.86
2009-01-03 01:00	-1.43
2009-01-04 09:00	-1.29
2009-01-05 10:00	-0.97
2009-01-06 11:00	-0.68
2009-01-04 12:00	-1.29
2009-01-05 13:00	-0.97
2009-01-06 14:00	-0.68
2009-01-01 20:00	-1.86
2009-01-02 21:00	-1.86

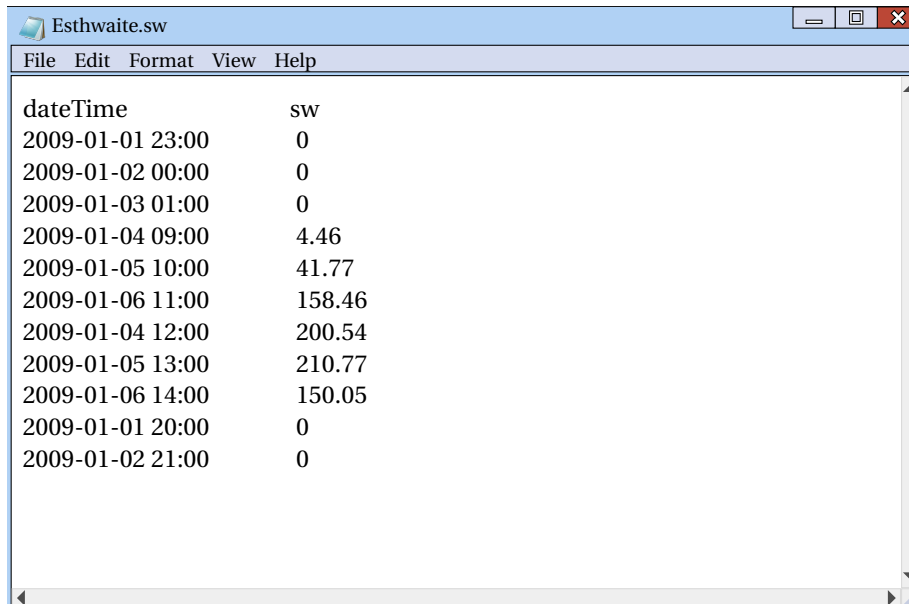
An example air temperature file used for Esthwaite Water.



A screenshot of a text editor window titled "Esthwaite.rh". The window has a menu bar with "File", "Edit", "Format", "View", and "Help". The text inside the window is as follows:

dateTime	rh
2009-01-01 23:00	96.37
2009-01-02 00:00	96.74
2009-01-03 01:00	96.53
2009-01-04 09:00	96.03
2009-01-05 10:00	95.47
2009-01-06 11:00	95.82
2009-01-04 12:00	96.03
2009-01-05 13:00	95.47
2009-01-06 14:00	95.82
2009-01-01 20:00	96.37
2009-01-02 21:00	96.74

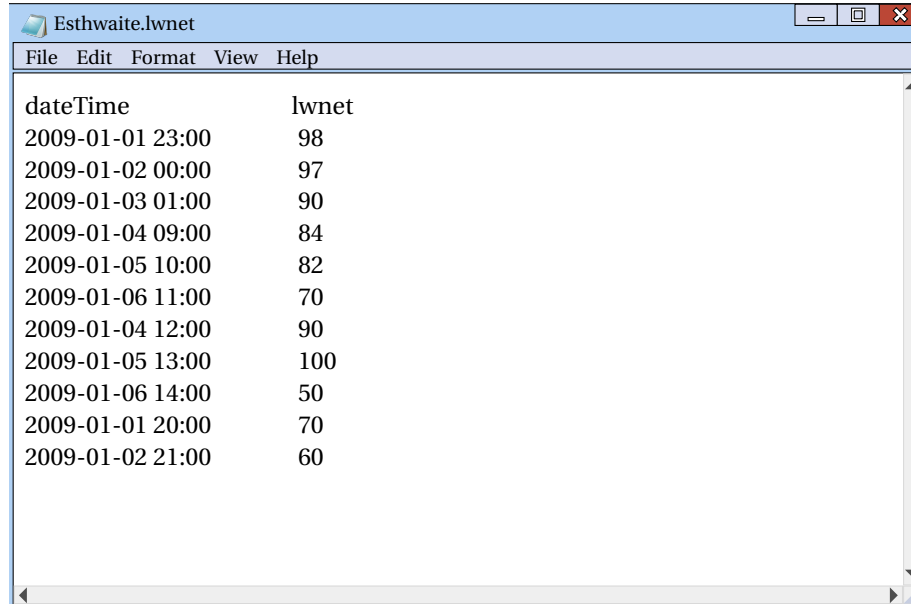
An example relative humidity file used for Esthwaite Water.



A screenshot of a text editor window titled "Esthwaite.sw". The window has a menu bar with "File", "Edit", "Format", "View", and "Help". The text inside the window is as follows:

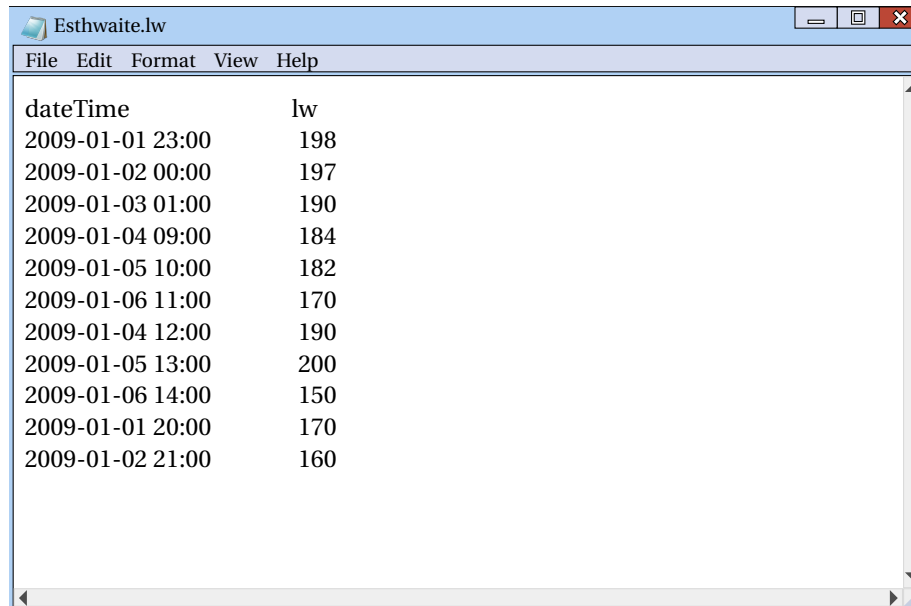
dateTime	sw
2009-01-01 23:00	0
2009-01-02 00:00	0
2009-01-03 01:00	0
2009-01-04 09:00	4.46
2009-01-05 10:00	41.77
2009-01-06 11:00	158.46
2009-01-04 12:00	200.54
2009-01-05 13:00	210.77
2009-01-06 14:00	150.05
2009-01-01 20:00	0
2009-01-02 21:00	0

An example short-wave radiation file used for Esthwaite Water.



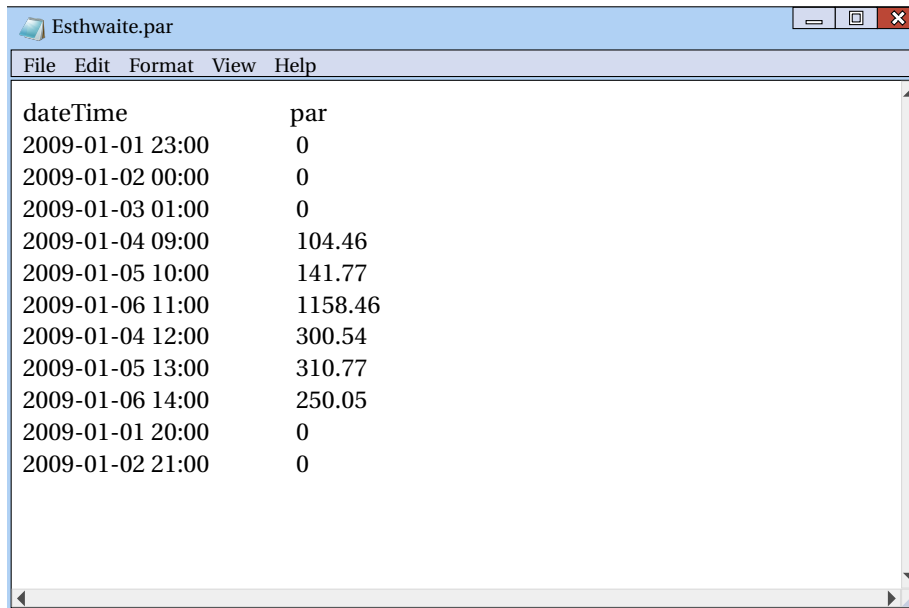
dateTime	lwnet
2009-01-01 23:00	98
2009-01-02 00:00	97
2009-01-03 01:00	90
2009-01-04 09:00	84
2009-01-05 10:00	82
2009-01-06 11:00	70
2009-01-04 12:00	90
2009-01-05 13:00	100
2009-01-06 14:00	50
2009-01-01 20:00	70
2009-01-02 21:00	60

An example net long-wave radiation file used for Esthwaite Water.



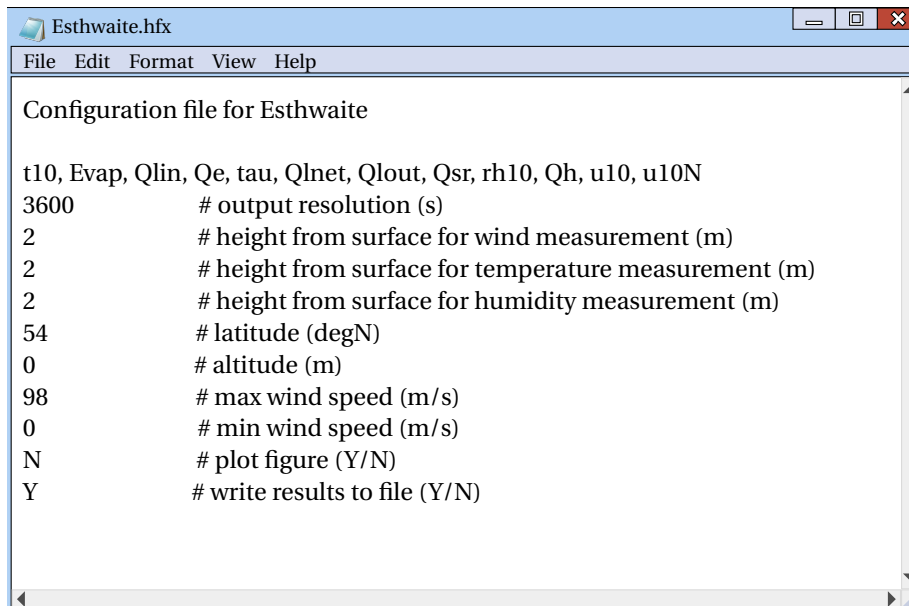
dateTime	lw
2009-01-01 23:00	198
2009-01-02 00:00	197
2009-01-03 01:00	190
2009-01-04 09:00	184
2009-01-05 10:00	182
2009-01-06 11:00	170
2009-01-04 12:00	190
2009-01-05 13:00	200
2009-01-06 14:00	150
2009-01-01 20:00	170
2009-01-02 21:00	160

An example incoming long-wave radiation file used for Esthwaite Water.



dateTime	par
2009-01-01 23:00	0
2009-01-02 00:00	0
2009-01-03 01:00	0
2009-01-04 09:00	104.46
2009-01-05 10:00	141.77
2009-01-06 11:00	1158.46
2009-01-04 12:00	300.54
2009-01-05 13:00	310.77
2009-01-06 14:00	250.05
2009-01-01 20:00	0
2009-01-02 21:00	0

An example photosynthetically active radiation file used for Esthwaite Water.



```

Configuration file for Esthwaite

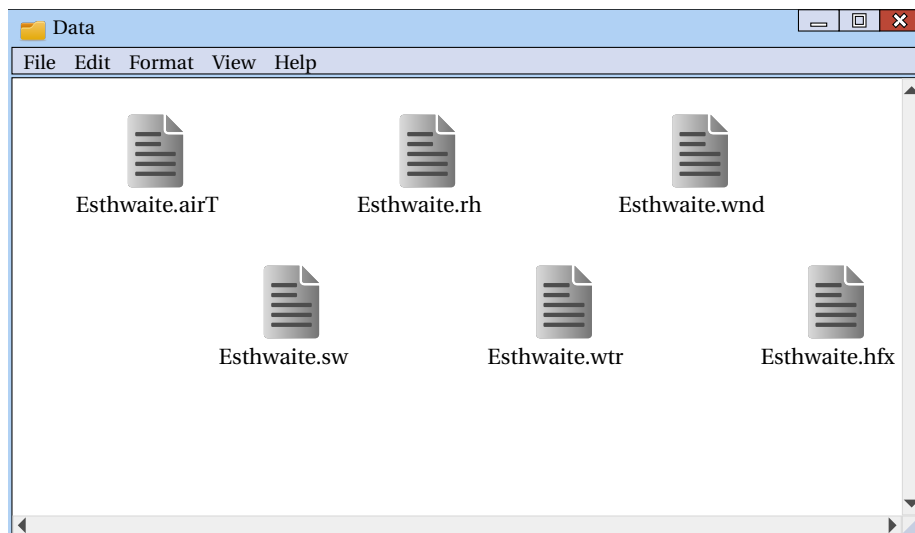
t10, Evap, Qlin, Qe, tau, Qlnet, Qlout, Qsr, rh10, Qh, u10, u10N
3600      # output resolution (s)
2         # height from surface for wind measurement (m)
2         # height from surface for temperature measurement (m)
2         # height from surface for humidity measurement (m)
54        # latitude (degN)
0         # altitude (m)
98        # max wind speed (m/s)
0         # min wind speed (m/s)
N         # plot figure (Y/N)
Y         # write results to file (Y/N)
  
```

An example configuration file used for Esthwaite Water (not all output options are shown)

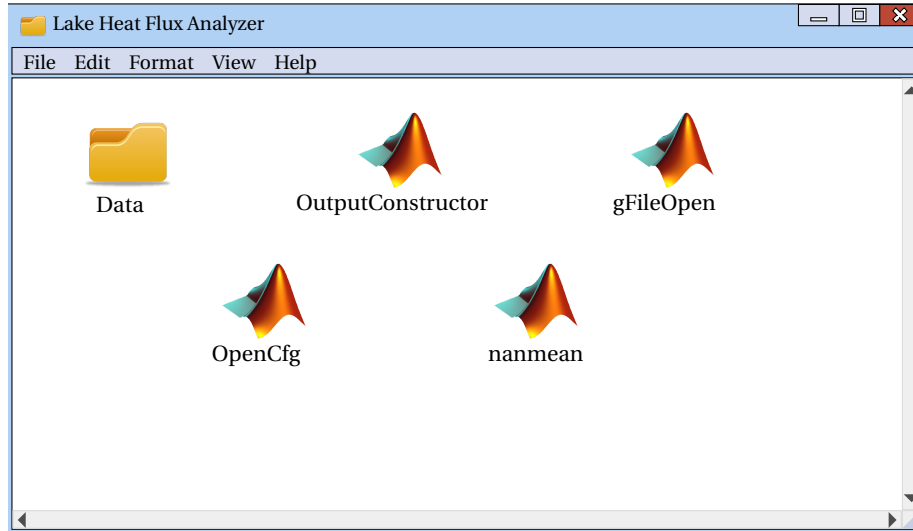
Chapter 2

Program operation

A step by step guide to Lake Heat Flux Analyzer is provided here.



Step 1: Set up the input files.



Step 2: Allocate the folder with inputs under the directory of Lake Heat Flux Analyzer.

```
Command Window
fx>> cd('C:\Lake Heat Flux Analyzer')
```

Step 3: Start MATLAB. Set the current directory to the folder where Lake Heat Flux Analyzer is saved.

```
Command Window
fx>> Run_LHFA('LakeName', 'FolderName')
```

Step 4: Initiate Lake Heat Flux Analyzer. LakeName is the file name shared among the input files, and the FolderName is the name of the folder that contains the input files. Configuration window will appear.

Output options

- Air shear velocity
- Air shear velocity neutral
- Air temperature at 10 m
- Atmospheric stability
- Evaporation
- Latent heat flux

Add

Output selections

- Water temperature

Remove

User parameters

output resolution (s) wind height (m)

temperature height (m) humidity height (m)

latitude (N) altitude (m)

max wind speed (m/s) min wind speed (m/s)

plot figure (Y/N) write results (Y/N)

☐ load from existing? **Publish**

Esthwaite.hfx preview

Configuration file for Esthwaite

```

wTemp #outputs
86400 #output resolution (s)
2 #height from surface for wind measurement (m)
2 #height from surface for temperature measurement (m)
2 #height from surface for humidity measurement (m)
54 # latitude (degN)
0 #altitude (m)
98 #max wind speed (m/s) inf if none
0.2 # min wind speed (m/s) -inf if none
Y #plot figure (Y/N)
Y #write results to file (Y/N)
    
```

Step 5: The configuration window automatically creates the configuration file (.hfx). Select the desired outputs and click ‘Add’. The selected outputs will then appear in both the ‘output selections’ and the ‘LakeName.hfx preview’ sections of the gui. Provide specific lake characteristics and then click ‘Publish’ to operate the program. When the analysis has successfully finished, the folder which the input files are located should contain a new results file. The output file has tab delimited format, thus the files can be viewed by Microsoft Excel or text editors. The user can also select ‘load from existing’, which will allow a previously generated configuration file to be used by the Lake Heat Flux Analyzer program.

```
Command Window
>> cd('C:\Lake Heat Flux Analyzer')

>> Run_LHFA('Esthwaite','Data')

Reading Esthwaite.hfx file ...completed

****Building program structure****

openWtr
openWnd
openRH
openAirT
openSW

****completed****

Reading Esthwaite.wtr file ...completed

Reading Esthwaite.wnd file ...completed

Reading Esthwaite.sw file ...completed

Reading Esthwaite.airT file ...completed

Reading Esthwaite.rh file ...completed

Writing results to file ...completed

Lake Heat Flux Analyzer is complete

fx>>
```

Example program run for Esthwaite Water, which will vary depending on the output selection. Lake Heat Flux Analyzer will only open the data files necessary for calculating the selected outputs.

heatfluxanalyzer.gleon.org

heatfluxanalyzer web

Web submit

Please zip your input files and upload them to run. An input example is provided to help you creat input of your own.

Inout files (zipped): No file chosen

Lake Heat Flux Analyzer has a web application heatfluxanalyzer.gleon.org which operates exactly the same way as the MATLAB application. The online application, however, does not show a configuration window, thus the user must prepare the configuration file (.hfx) prior to the program operation. Please follow the examples shown in Chapter 1 to create the configuration file. All the input files should have common names. The input files should be zipped into one file and the zip file must share its name with the other input files. An example file for Esthwaite Water can be found on the website. Once the input files are prepared, the file name and its location should be chosen by following the instructions on the website.

Chapter 3

Bulk parameterization of surface fluxes

The following section describes the algorithm developed for estimating the surface energy fluxes from lake buoy data. We describe the methods used for calculating the reflected short-wave radiation (Q_{sr}), the sensible (Q_h) and latent (Q_e) heat fluxes, the incoming long-wave (Q_{lin}) and the outgoing long-wave radiation (Q_{lout}), expressed in terms of the total surface heat flux (Q_{tot}) as

$$Q_{tot} = Q_{sin} + Q_{lin} - Q_{lout} - Q_e - Q_h, \quad (3.1)$$

where Q_{sin} is the net incoming short-wave radiation (W m^{-2}), Q_{lin} is the incoming long-wave radiation (W m^{-2}), Q_{lout} is the outgoing long-wave radiation (W m^{-2}), Q_e is the latent heat flux (W m^{-2}), and Q_h is the sensible heat flux (W m^{-2}). To calculate these fluxes, a variety of input variables

are required: surface water temperature, air temperature (T_z) at height z_t (m) above the water surface ($^{\circ}\text{C}$), relative humidity (R_h) at height z_q (m) above the water surface (%), wind speed (u_z) at height z_u (m) above the water surface (m s^{-1}), and short-wave radiation (Q_s) measured at the lake surface (W m^{-2}). In addition, the measurement height of the sensors above the water surface is needed.

3.1 Incident and reflected short-wave radiation

The amount of short-wave radiation reaching the lake surface can be measured directly, using relatively inexpensive radiometers. The short-wave albedo, α_{sw} , however, influences the amount of radiation that is reflected back to the atmosphere, and thus influences the amount of radiation that penetrates beneath the water surface. Incoming short-wave radiation, Q_{sin} (W m^{-2}), by taking the short-wave albedo into account, can be expressed as:

$$Q_{sin} = Q_s (1 - \alpha_{sw}). \quad (3.2)$$

Here, α_{sw} is estimated from Fresnel's equation as:

$$\alpha_{sw} = \frac{1}{2} \left[\frac{\tan^2 (Z - R_{ref})}{\tan^2 (Z + R_{ref})} + \frac{\sin^2 (Z - R_{ref})}{\sin^2 (Z + R_{ref})} \right], \quad (3.3)$$

where R_{ref} is the angle of refraction calculated from Snell's law as:

$$R_{ref} = \sin^{-1} \left(\frac{\sin(Z)}{\eta} \right), \quad (3.4)$$

where $\eta = 1.33$ is the index of refraction (Kirk, 1994) and Z is the solar zenith angle calculated as a function of latitude (φ), solar declination (δ) and the hour angle (H) as:

$$Z = \cos^{-1} \left(\sin \left(\frac{2\varphi\pi}{360} \right) \sin \left(\frac{2\delta\pi}{360} \right) + \cos \left(\frac{2\varphi\pi}{360} \right) \cos \left(\frac{2\delta\pi}{360} \right) \cos H \right), \quad (3.5)$$

$$\begin{aligned} \delta = \frac{180}{\pi} & (0.006918 - 0.399912 \cos(\gamma) + 0.070257 \sin \gamma \\ & - 0.006758 \cos 2\gamma + 0.000907 \sin 2\gamma - 0.002697 \cos 3\gamma \\ & + 0.00148 \sin 3\gamma), \end{aligned} \quad (3.6)$$

$$\gamma = 2\pi (DOY - 1) / 365, \quad (3.7)$$

$$H = (\pi/12) (t_{noon} - t_{solar}), \quad (3.8)$$

where DOY is the decimal day of year (e.g. Jan 10th = 10), t_{noon} is the local solar noon and t_{solar} is local solar time.

3.2 Long-wave radiation

The net long-wave heat flux (W m^{-2}) across the air-water interface comprises two main components: (i) incoming long-wave radiation and (ii) outgoing

long-wave radiation. The bulk formulae may be expressed as:

$$Q_{lnet} = Q_{lin} - Q_{lout}, \quad (3.9)$$

where in the absence of direct measurements, these are estimated from frequently measured variables.

In this program outgoing long-wave radiation is estimated as:

$$Q_{lout} = \varepsilon_w \sigma T_{0K}^4, \quad (3.10)$$

where $\varepsilon_w = 0.972$ (Davies et al., 1971) is the emissivity of water, $\sigma = 5.67 \times 10^{-8}$ is the Stefan-Boltzmann constant ($\text{W m}^{-2} \text{K}^{-4}$), and T_{0K} is the surface water temperature in Kelvin. Incoming long-wave radiation is estimated following the methods of Crawford and Duchon (1999) as used in other limnological studies (e.g. Jakkila et al., 2009; Read et al., 2012). Following this method, the incoming long-wave radiation can be estimated as:

$$Q_{lin} = \left\{ clf + (1 - clf) \left(1.22 + 0.06 \sin \left[(\text{month} + 2) \frac{\pi}{6} \right] \right) \left(\frac{e_z}{T_{zK}} \right)^{1/7} \right\} \sigma T_{zK}^4, \quad (3.11)$$

where month is the numerical month (e.g. January = 1), T_{zK} is air temperature in Kelvin, and e_z is the vapour pressure of the air (hPa) calculated as $e_z = R_h E_s$ where E_s is the saturation vapour pressure estimated based on the saturation vapour pressure of the air calculated following Lowe (1977)

as:

$$E_s = a_0 + T_z (a_1 + T_z (a_2 + T_z (a_3 + T_z (a_4 + T_z (a_5 + a_6 T_z))))), \quad (3.12)$$

where a_0 to a_6 ($^{\circ}\text{C}$) are given by:

$$\begin{aligned} a_0 &= 6.107799961, \\ a_1 &= 4.436518521 \times 10^{-1}, \\ a_2 &= 1.428945805 \times 10^{-2}, \\ a_3 &= 2.650648471 \times 10^{-4}, \\ a_4 &= 3.031240396 \times 10^{-6}, \\ a_5 &= 2.034080948 \times 10^{-8}, \\ a_6 &= 6.136820929 \times 10^{-11}. \end{aligned}$$

The cloud cover fraction, clf , is estimated as:

$$clf = 1 - s, \quad (3.13)$$

where s is the ratio of the measured short-wave radiation (i.e. Q_s) to the clear-sky short-wave radiation, I_c . The clear-sky short-wave radiation is estimated as:

$$I_c = I_{eff} (\cos Z) T_R T_{pg} T_w T_a, \quad (3.14)$$

CHAPTER 3. BULK PARAMETERIZATION OF SURFACE FLUXES

where I_{eff} is the effective solar constant, calculated following (Meyers and Dale, 1983) as:

$$I_{eff} = 1353 \{1 + 0.034 \times \cos [2\pi (DOY - 1) / 365]\}, \quad (3.15)$$

and T_i represent the transmission coefficients for Rayleigh scattering (R), absorption by permanent gases (pg) and water vapour (w), and absorption and scattering by aerosols (a).

An empirical relationship to account for the effects of Rayleigh scattering and absorption by permanent gases was given by Kondratyev (1969). Atwater and Brown (1974) later modified this expression to account for the isotropic nature of Rayleigh scattering with one-half of the scattered radiation being in the forward direction. This formula may be expressed as:

$$T_R T_{pg} = 1.021 - 0.084 [m (0.000949p + 0.051)]^{0.5}, \quad (3.16)$$

where p is the surface pressure (mb) calculated as a function of altitude as:

$$p = \left[101325 (1 - \text{altitude} \times 2.25577 \times 10^{-5})^{5.25588} \right] / 100, \quad (3.17)$$

and m is the air mass thickness coefficient, calculated as:

$$m = 35 \cos Z (1244 \cos^2 Z + 1)^{-0.5}, \quad (3.18)$$

CHAPTER 3. BULK PARAMETERIZATION OF SURFACE FLUXES

where $\cos Z$ is the cosine of the solar zenith angle (equation 3.5). A formula by McDonald (1960) is used to account for water vapour absorption in the atmosphere, T_w , which may be calculated as:

$$T_w = 1 - 0.077 (pw \times m)^{0.3}, \quad (3.19)$$

where pw is the precipitable water which is estimated as:

$$pw = \exp [(0.1133 - \ln (G + 1)) + 0.0393T_d], \quad (3.20)$$

T_d ($^{\circ}\text{F}$) is the dew point temperature estimated as:

$$T_d = \frac{[243.5 \times \ln (e_z/6.112)]}{[17.67 - \ln (e_z/6.112)]} + 33.8, \quad (3.21)$$

and G is an empirically-derived constant for different seasons and latitudes (Table 3.1).

As standard meteorological observations cannot be used to estimate the aerosol attenuation, T_a is calculated as a residual from clear sky conditions. The relation follows an expression given by Houghton (1954) which is:

$$T_a = 0.95^m. \quad (3.22)$$

Once I_c was calculated from equation 3.14, direct observations of solar irradiance were then used to calculate s and clf in equation 3.13. As clf increases

Table 3.1 Seasonal and latitudinal mean values of G (Smith, 1966).

Latitudinal zone ($^{\circ}$)	Winter	Spring	Summer	Autumn	Annual average
0-10	3.37	2.85	2.80	2.64	2.91
10-20	2.99	3.02	2.70	2.93	2.91
20-30	3.60	3.00	2.98	2.93	3.12
30-40	3.04	3.11	2.92	2.94	3.00
40-50	2.70	2.95	2.77	2.71	2.78
50-60	2.52	3.07	2.67	2.93	2.79
60-70	1.76	2.69	2.61	2.61	2.41
70-80	1.60	1.67	2.24	2.63	2.03
80-90	1.11	1.44	1.94	2.02	1.62

from 0 to 1, calculated values of clf less than zero are adjusted back to zero to be physically realistic (Crawford and Duchon, 1999).

As the calculation of incoming long-wave radiation is based on the ratio of clear-sky and measured short-wave radiation, incoming long-wave radiation cannot be calculated at night. In this program, night-time incoming long-wave radiation values are estimated as the mean of the daytime values. This adds an additional source of uncertainty in these estimates, but in comparison to more widely-used incoming long-wave formulae (e.g. Gill, 1982), which are daily averages, this method has been shown to provide a more accurate representation of incoming long-wave radiation (Crawford and Duchon, 1999).

3.3 Bulk algorithms for momentum, sensible and latent heat fluxes

The air-water fluxes of momentum (τ , N m^{-2}), heat (Q_h , W m^{-2}), and moisture (Q_e , W m^{-2}) are parametrized by bulk algorithms that relate surface layer data to surface fluxes using formulae based on similarity theory and empirical relationships. The standard procedure involves the calculation of roughness lengths for momentum, heat, and moisture (z_o , z_{oh} , z_{oq}) and the corresponding transfer coefficients (C_d , C_h , C_e) from observed wind speed (u), temperature (T), and humidity (q) profiles, via an iteration routine involving a friction velocity term u_{*a} , a scaling potential temperature T_* , and a scaling humidity q_* . Using the above terms, surface fluxes for momentum, sensible heat, and latent heat can be calculated as:

$$\tau = C_{dz}\rho_z u_z^2 = \rho_z u_{*a}^2, \quad (3.23)$$

$$Q_h = \rho_z C_{pa} C_{hz} u_z (T_0 - T_z) = -\rho_z C_{pa} u_{*a} T_*, \quad (3.24)$$

$$Q_e = \rho_z L_v C_{ez} u_z (q_0 - q_z) = -\rho_z L_v u_{*a} q_*, \quad (3.25)$$

where $\rho_z = 100p/[R_a(T_z + 273.16)]$ is the density (kg m^{-3}) of the overlying air (Verburg and Antenucci, 2010), and $R_a = 287(1 + 0.608q_z)$ is the gas constant for moist air ($\text{J kg}^{-1} \text{ }^\circ\text{C}^{-1}$); $C_{pa} = 1006$ is the specific heat of air at constant pressure ($\text{J kg}^{-1} \text{ }^\circ\text{C}^{-1}$); $L_v = 2.501 \times 10^6 - 2370 \times T_0$ is the latent heat of vaporisation (J kg^{-1}); $q_0 = 0.622 \times e_{sat}/[p + (0.622 - 1)e_{sat}]$

is the specific humidity at saturation pressure (kg kg^{-1}), e_{sat} is the saturated vapour pressure (hPa) calculated following Bolton (1980) as $e_{sat} = 6.11 \exp [17.27T_0 / (237.3 + T_0)]$; $q_z = 0.622 \times e_z / [p + (0.622 - 1) e_z]$ is the specific humidity of the air (kg kg^{-1}) at height z_q (m) above the water surface, $e_z = R_h e_s / 100$, and $e_s = 6.11 \exp [17.27T_z / 237.3 + T_z]$ is the saturated vapour pressure (hPa) at z_t . Here, C_{dz} , C_{hz} and C_{ez} are transfer coefficients for heights z_u , z_t and z_q , respectively.

A variety of bulk flux algorithms are presently used in the literature (e.g. Fairall et al., 2003, 1996; Verburg and Antenucci, 2010; Zeng et al., 1998). While these algorithms all use equations (3.23) to (3.25) to calculate the surface fluxes, they differ in the parameterization of the transfer coefficients, the treatment of free convective conditions and surface layer gustiness. In this program the turbulent fluxes were calculated following Zeng et al. (1998), which applies Monin-Obukhov similarity theory to the atmospheric boundary layer. This theory states that wind, temperature and humidity profile gradients depend on unique functions of the stability parameter, ζ , where $\zeta = zL_w^{-1}$:

$$\frac{\kappa z_u}{u_{*a}} \frac{du}{dz} = \phi_m(\zeta), \quad \frac{\kappa z_t}{T_*} \frac{dT}{dz} = \phi_h(\zeta), \quad \frac{\kappa z_q}{q_*} \frac{dq}{dz} = \phi_e(\zeta), \quad (3.26)$$

where L_w is the Monin-Obukhov length scale (m), κ is the von Karman constant ($= 0.41$), and ϕ_m , ϕ_h and ϕ_e are the similarity functions that relate the fluxes of momentum, heat, and moisture to the mean profile gradients

of wind, temperature and humidity, respectively. According to Brutsaert (1982), the Monin-Obukhov length scale is a measure of the ratio of the reduction of potential energy due to wind mixing and the growth of atmospheric stratification due to surface fluxes and may be calculated following Monin and Obukhov (1954) as:

$$L_w = \frac{-\rho_z u_{*a}^3 T_v}{\kappa g \left(\frac{Q_h}{C_{pa}} + 0.61 \times \frac{(T_z + 273.16) Q_e}{L_v} \right)}, \quad (3.27)$$

where $T_v = (T_z + 273.16) \times (1 + 0.61 q_z)$ is the virtual air temperature (K) and $g = 9.78033 \left(1 + (0.0053 \sin^2 |\varphi| - 5.8 \times 10^{-6} \sin^2 |\varphi|) \right)$ is the gravitational acceleration (m s^{-2}), where the standard value of 9.81 m s^{-2} is given at latitude $\sim 45.5^\circ$.

Following Zeng et al. (1998), the differential equations for ϕ_m , ϕ_h and ϕ_e can be integrated between the roughness length and the measurement height to obtain wind, temperature and moisture gradients in the atmospheric boundary layer and the corresponding scaling parameters used in calculating the turbulent surface fluxes. The roughness length of momentum (z_o) was calculated following Smith (1998) as:

$$z_o = \left(\frac{\alpha_1 u_{*a}^2}{g} \right) + \left(\frac{\alpha_2 v_a}{u_{*a}} \right), \quad (3.28)$$

where α_1 is the Charnock constant ($= 0.013$), $\alpha_2 = 0.11$, and v_a is the kinematic viscosity of air ($= 1.5 \times 10^{-5} \text{ m}^2 \text{ s}^{-1}$). The functional form of

CHAPTER 3. BULK PARAMETERIZATION OF SURFACE FLUXES

Brutsaert (1982) is then used to estimate the roughness length of heat (z_{ot}) and humidity (z_{oq}) as:

$$z_{oq} = z_{ot} = z_o \exp \left(-b_1 Re^{0.25} - b_2 \right), \quad (3.29)$$

where $b_1 = 2.67$, $b_2 = -2.57$, and $Re = u_{*a} z_o / \nu_a$ is the roughness Reynolds number.

Using the Monin-Obukhov similarity theory, the flux-gradient relations for momentum, $\phi_m(\zeta)$, are:

$$\phi_m(\zeta) = 5 + \zeta \quad \text{for} \quad \zeta > 1 \text{ (very stable)} \quad (3.30)$$

$$\phi_m(\zeta) = 1 + 5\zeta \quad \text{for} \quad 0 \leq \zeta \leq 1 \text{ (stable)} \quad (3.31)$$

$$\phi_m(\zeta) = (1 - 16\zeta)^{-1/4} \quad \text{for} \quad -1.574 \leq \zeta < 0 \text{ (unstable)} \quad (3.32)$$

$$\phi_m(\zeta) = (0.7\kappa^{2/3}) (-\zeta)^{1/3} \quad \text{for} \quad \zeta < -1.574 \text{ (very unstable)} \quad (3.33)$$

and for sensible and latent heat, where $\phi_e(\zeta) = \phi_h(\zeta)$, are:

$$\phi_e(\zeta) = 5 + \zeta \quad \text{for} \quad \zeta > 1 \text{ (very stable)} \quad (3.34)$$

$$\phi_e(\zeta) = 1 + 5\zeta \quad \text{for} \quad 0 \leq \zeta \leq 1 \text{ (stable)} \quad (3.35)$$

$$\phi_e(\zeta) = (1 - 16\zeta)^{-1/2} \quad \text{for} \quad -0.465 \leq \zeta < 0 \text{ (unstable)} \quad (3.36)$$

$$\phi_e(\zeta) = 0.9\kappa^{4/3} (-\zeta)^{-1/3} \quad \text{for} \quad \zeta < -0.465 \text{ (very unstable)} \quad (3.37)$$

CHAPTER 3. BULK PARAMETERIZATION OF SURFACE FLUXES

where to ensure continuous functions of $\phi_m(\zeta)$, $\phi_h(\zeta)$ and $\phi_e(\zeta)$ we can match the relations for very unstable conditions at $\zeta_m = -1.574$ for $\phi_m(\zeta)$ and $\zeta_h = \zeta_e = -0.465$ for $\phi_h(\zeta) = \phi_e(\zeta)$. The flux gradient relations can then be integrated to yield wind profiles, and the corresponding friction velocity, u_{*a} , as:

$$\phi_m = \frac{\kappa z_u}{u_{*a}} \frac{du}{dz} = 5 + \zeta, \quad (3.38)$$

$$\phi_m = \frac{\kappa z_u}{u_{*a}} \frac{du}{dz} = 5 + \left(\frac{z_u}{L_w} \right),$$

and then by re-arranging for du and integrating between z_o and z_u we obtain

$$\begin{aligned} du &= \frac{u_{*a}}{\kappa} \left\{ \left(\ln \left(\frac{L_w}{z_o} \right) + 5 \right) + \left[5 \ln \left(\frac{z_u}{L_w} \right) + \left(\frac{z_u}{L_w} \right) - 1 \right] \right\}, \\ u_z - u_0 &= \frac{u_{*a}}{\kappa} \left\{ \left(\ln \left(\frac{L_w}{z_o} \right) + 5 \right) + \left[5 \ln \left(\frac{z_u}{L_w} \right) + \left(\frac{z_u}{L_w} \right) - 1 \right] \right\}, \\ u_z &= \frac{u_{*a}}{\kappa} \left\{ \left(\ln \left(\frac{L_w}{z_o} \right) + 5 \right) + \left[5 \ln \left(\frac{z_u}{L_w} \right) + \left(\frac{z_u}{L_w} \right) - 1 \right] \right\}, \end{aligned} \quad (3.39)$$

$$u_{*a} = u_z \kappa \left\{ \left(\ln \left(\frac{L_w}{z_o} \right) + 5 \right) + \left[5 \ln \left(\frac{z_u}{L_w} \right) + \left(\frac{z_u}{L_w} \right) - 1 \right] \right\}^{-1}, \quad (3.40)$$

$$u_{10} = \frac{u_{*a}}{\kappa} \left\{ \left(\ln \left(\frac{L_w}{z_o} \right) + 5 \right) + \left[5 \ln \left(\frac{10}{L_w} \right) + \left(\frac{10}{L_w} \right) - 1 \right] \right\}, \quad (3.41)$$

for very stable conditions ($\zeta > 1$),

$$\phi_m = \frac{\kappa z_u}{u_{*a}} \frac{du}{dz} = 1 + 5\zeta, \quad (3.42)$$

$$\phi_m = \frac{\kappa z_u}{u_{*a}} \frac{du}{dz} = 1 + 5 \left(\frac{z_u}{L_w} \right),$$

and then by re-arranging for du and integrating between z_o and z_u we obtain

$$\begin{aligned} du &= \frac{u_{*a}}{\kappa} \left[\ln \left(\frac{z_u}{z_o} \right) + 5 \left(\frac{z_u}{L_w} \right) \right], \\ u_z - u_0 &= \frac{u_{*a}}{\kappa} \left[\ln \left(\frac{z_u}{z_o} \right) + 5 \left(\frac{z_u}{L_w} \right) \right], \\ u_z &= \frac{u_{*a}}{\kappa} \left[\ln \left(\frac{z_u}{z_o} \right) + 5 \left(\frac{z_u}{L_w} \right) \right], \end{aligned} \quad (3.43)$$

$$u_{*a} = u_z \kappa \left[\ln \left(\frac{z_u}{z_o} \right) + 5 \left(\frac{z_u}{L_w} \right) \right]^{-1}, \quad (3.44)$$

$$u_{10} = \frac{u_{*a}}{\kappa} \left[\ln \left(\frac{10}{z_o} \right) + 5 \left(\frac{10}{L_w} \right) \right], \quad (3.45)$$

for stable conditions ($0 < \zeta < 1$),

$$\phi_m = \frac{\kappa z_u}{u_{*a}} \frac{du}{dz} = \left[1 - 16\zeta \right]^{-1/4}, \quad (3.46)$$

$$\phi_m = \frac{\kappa z_u}{u_{*a}} \frac{du}{dz} = \left[1 - 16 \left(\frac{z_u}{L_w} \right) \right]^{-1/4},$$

and then by re-arranging for du and integrating between z_o and z_u we obtain

$$\begin{aligned} du &= \frac{u_{*a}}{\kappa} \left[\ln \left(\frac{z_u}{z_o} \right) - \psi_m \left(\frac{z_u}{L_w} \right) \right], \\ u_z - u_0 &= \frac{u_{*a}}{\kappa} \left[\ln \left(\frac{z_u}{z_o} \right) - \psi_m \left(\frac{z_u}{L_w} \right) \right], \\ u_z &= \frac{u_{*a}}{\kappa} \left[\ln \left(\frac{z_u}{z_o} \right) - \psi_m \left(\frac{z_u}{L_w} \right) \right], \end{aligned} \quad (3.47)$$

$$u_{*a} = u_z \kappa \left[\ln \left(\frac{z_u}{z_o} \right) - \psi_m \left(\frac{z_u}{L_w} \right) \right]^{-1}, \quad (3.48)$$

$$u_{10} = \frac{u_{*a}}{\kappa} \left[\ln \left(\frac{10}{z_o} \right) - \psi_m \left(\frac{10}{L_w} \right) \right], \quad (3.49)$$

for unstable conditions ($\zeta_m < \zeta < 0$), and

$$\phi_m = \frac{\kappa z_u}{u_{*a}} \frac{du}{dz} = (0.7 \kappa^{2/3}) (-\zeta)^{1/3}, \quad (3.50)$$

$$\phi_m = \frac{\kappa z_u}{u_{*a}} \frac{du}{dz} = \left(0.7 \kappa^{2/3} \right) \left(-\frac{z_u}{L_w} \right)^{1/3},$$

and then by re-arranging for du and integrating between z_o and z_u we obtain

$$du = \frac{u_{*a}}{\kappa} \left\{ \left[\ln \left(\frac{\zeta_m L_w}{z_o} \right) - \psi_m(\zeta_m) \right] \right\}$$

$$\begin{aligned}
 & + 1.14 \left[\left(-\frac{z_u}{L_w} \right)^{1/3} - (-\zeta_m)^{1/3} \right] \Bigg\}, \\
 u_z - u_0 &= \frac{u_{*a}}{\kappa} \left\{ \left[\ln \left(\frac{\zeta_m L_w}{z_o} \right) - \psi_m(\zeta_m) \right] \right. \\
 & \quad \left. + 1.14 \left[(-\zeta_m)^{1/3} - (-\zeta_m)^{1/3} \right] \right\}, \\
 u_z &= \frac{u_{*a}}{\kappa} \left\{ \left[\ln \left(\frac{\zeta_m L_w}{z_o} \right) - \psi_m(\zeta_m) \right] \right. \\
 & \quad \left. + 1.14 \left[(-\zeta_m)^{1/3} - (-\zeta_m)^{1/3} \right] \right\}, \tag{3.51}
 \end{aligned}$$

$$\begin{aligned}
 u_{*a} &= u_z \kappa \left\{ \left[\ln \left(\frac{\zeta_m L_w}{z_o} \right) - \psi_m(\zeta_m) \right] \right. \\
 & \quad \left. + 1.14 \left[\left(-\frac{z_u}{L_w} \right) - (-\zeta_m)^{1/3} \right] \right\}^{-1}, \tag{3.52}
 \end{aligned}$$

$$\begin{aligned}
 u_{10} &= \frac{u_{*a}}{\kappa} \left\{ \left[\ln \left(\frac{\zeta_m L_w}{z_o} \right) - \psi_m(\zeta_m) \right] \right. \\
 & \quad \left. + 1.14 \left[\left(-\frac{10}{L_w} \right)^{1/3} - (-\zeta_m)^{1/3} \right] \right\}, \tag{3.53}
 \end{aligned}$$

for very unstable conditions ($\zeta < \zeta_m = -1.574$) where

$$\psi_m(\zeta) = 2 \ln \left(\frac{1 + \chi}{2} \right) + \ln \left(\frac{1 + \chi^2}{2} \right) - 2 \tan^{-1} \chi + \frac{\pi}{2}, \tag{3.54}$$

is the stability function for momentum under stable conditions and

$$\chi = (1 - 16\zeta)^{1/4}. \tag{3.55}$$

CHAPTER 3. BULK PARAMETERIZATION OF SURFACE FLUXES

Under stable conditions ($\zeta > 0$), the wind speed u_z is defined as:

$$u_z = \max [u_z, 0.1], \quad (3.56)$$

and for unstable cases ($\zeta < 0$), u_z is given by:

$$u_z = [u_z^2 + (\beta_* w_{*a})^2]^{1/2}, \quad (3.57)$$

where w_{*a} is the convective velocity scale in the atmospheric boundary layer, defined as:

$$w_{*a} = \left(-\frac{g}{T_v} T_{v*} u_{*a} z_i \right)^{1/3}, \quad (3.58)$$

where z_i is the convective boundary layer height ($= 1000$ m), $\beta_* = 1$, and T_{v*} is the virtual potential temperature scaling parameter, calculated as:

$$T_{v*} = T_* (1 + 0.61 q_z / 100) + 0.61 \times T_h, \quad (3.59)$$

where $T_h = (T_z + 273.16) \times (100/p)^{(287.1/1004.67)}$ is the potential temperature, which is the temperature that a parcel of air would acquire if it was adiabatically brought to a standard reference pressure. The flux gradient relations for heat follow a similar manner to that of wind, but by integrating the flux gradients for heat we obtain

$$\phi_h = \frac{\kappa z_t}{T_*} \frac{dT}{dz} = 5 + \zeta, \quad (3.60)$$

$$\phi_h = \frac{\kappa z_t}{T_*} \frac{dT}{dz} = 5 + \left(\frac{z_t}{L_w} \right),$$

and then by re-arranging for dT and integrating between z_{ot} and z_t we obtain

$$\begin{aligned} dT &= \frac{T_*}{\kappa} \left\{ \left[\ln \left(\frac{L_w}{z_{ot}} \right) + 5 \right] + \left[5 + \ln \left(\frac{z_t}{L_w} \right) + \left(\frac{z_t}{L_w} \right) - 1 \right] \right\}, \\ T_z - T_0 &= \frac{T_*}{\kappa} \left\{ \left[\ln \left(\frac{L_w}{z_{ot}} \right) + 5 \right] + \left[5 + \ln \left(\frac{z_t}{L_w} \right) + \left(\frac{z_t}{L_w} \right) - 1 \right] \right\}, \\ T_z &= \frac{T_*}{\kappa} \left\{ \left[\ln \left(\frac{L_w}{z_{ot}} \right) + 5 \right] + \left[5 + \ln \left(\frac{z_t}{L_w} \right) + \left(\frac{z_t}{L_w} \right) - 1 \right] \right\} + T_0, \end{aligned} \quad (3.61)$$

$$T_* = T_z \kappa \left\{ \left\{ \left[\ln \left(\frac{L_w}{z_{ot}} \right) + 5 \right] + \left[5 + \ln \left(\frac{z_t}{L_w} \right) + \left(\frac{z_t}{L_w} \right) - 1 \right] \right\} + T_0 \right\}^{-1}, \quad (3.62)$$

$$T_{10} = \frac{T_*}{\kappa} \left\{ \left[\ln \left(\frac{L_w}{z_{ot}} \right) + 5 \right] + \left[5 + \ln \left(\frac{10}{L_w} \right) + \left(\frac{10}{L_w} \right) - 1 \right] \right\} + T_0, \quad (3.63)$$

for very stable conditions ($\zeta > 1$),

$$\phi_h = \frac{\kappa z_t}{T_*} \frac{dT}{dz} = 1 + 5\zeta, \quad (3.64)$$

$$\phi_h = \frac{\kappa z_t}{T_*} \frac{dT}{dz} = 1 + 5 \left(\frac{z_t}{L_w} \right),$$

and then by re-arranging for dT and integrating between z_{ot} and z_t we obtain

$$\begin{aligned} dT &= \frac{T_*}{\kappa} \left[\ln \left(\frac{z_t}{z_{ot}} \right) + 5 \left(\frac{z_t}{L_w} \right) \right], \\ T_z - T_0 &= \frac{T_*}{\kappa} \left[\ln \left(\frac{z_t}{z_{ot}} \right) + 5 \left(\frac{z_t}{L_w} \right) \right], \\ T_z &= \frac{T_*}{\kappa} \left[\ln \left(\frac{z_t}{z_{ot}} \right) + 5 \left(\frac{z_t}{L_w} \right) \right] + T_0, \end{aligned} \quad (3.65)$$

$$T_* = T_z \kappa \left\{ \left[\ln \left(\frac{z_t}{z_{ot}} \right) + 5 \left(\frac{z_t}{L_w} \right) \right] + T_0 \right\}^{-1}, \quad (3.66)$$

$$T_{10} = \frac{T_*}{\kappa} \left[\ln \left(\frac{10}{z_{ot}} \right) + 5 \left(\frac{10}{L_w} \right) \right] + T_0, \quad (3.67)$$

for stable conditions ($0 < \zeta < 1$),

$$\phi_h = \frac{\kappa z_t}{T_*} \frac{dT}{dz} = (1 - 16\zeta)^{-1/2}, \quad (3.68)$$

$$\phi_h = \frac{\kappa z_t}{T_*} \frac{dT}{dz} = \left(1 - 16 \left(\frac{z_t}{L_w} \right) \right)^{-1/2},$$

and then by re-arranging for dT and integrating between z_{ot} and z_t we obtain

$$\begin{aligned} dT &= \frac{T_*}{\kappa} \left[\ln \left(\frac{z_t}{z_{ot}} \right) - \psi_h \left(\frac{z_t}{L_w} \right) \right], \\ T_z - T_0 &= \frac{T_*}{\kappa} \left[\ln \left(\frac{z_t}{z_{ot}} \right) - \psi_h \left(\frac{z_t}{L_w} \right) \right], \end{aligned}$$

$$T_z = \frac{T_*}{\kappa} \left[\ln \left(\frac{z_t}{z_{ot}} \right) - \psi_h \left(\frac{z_t}{L_w} \right) \right] + T_0, \quad (3.69)$$

$$T_* = T_z \kappa \left\{ \left[\ln \left(\frac{z_t}{z_{ot}} \right) - \psi_h \left(\frac{z_t}{L_w} \right) \right] + T_0 \right\}^{-1}, \quad (3.70)$$

$$T_{10} = \frac{T_*}{\kappa} \left[\ln \left(\frac{10}{z_{ot}} \right) - \psi_h \left(\frac{10}{L_w} \right) \right] + T_0, \quad (3.71)$$

for unstable conditions ($\zeta_h < \zeta < 0$), and

$$\phi_h = \frac{\kappa z_t}{T_*} \frac{dT}{dz} = 0.9 \kappa^{4/3} (-\zeta)^{-1/3}, \quad (3.72)$$

$$\phi_h = \frac{\kappa z_t}{T_*} \frac{dT}{dz} = 0.9 \kappa^{4/3} \left(-\frac{z_t}{L_w} \right)^{-1/3}, \quad (3.73)$$

and then by re-arranging for dT and integrating between z_{ot} and z_t we obtain

$$\begin{aligned} dT &= \frac{T_*}{\kappa} \left\{ \left[\ln \left(\frac{\zeta_h L_w}{z_{ot}} \right) - \psi_h(\zeta_h) \right] \right. \\ &\quad \left. + 0.8 \left[(-\zeta_h)^{-1/3} - \left(-\frac{z_t}{L_w} \right)^{-1/3} \right] \right\}, \\ T_z - T_0 &= \frac{T_*}{\kappa} \left\{ \left[\ln \left(\frac{\zeta_h L_w}{z_{ot}} \right) - \psi_h(\zeta_h) \right] \right. \\ &\quad \left. + 0.8 \left[(-\zeta_h)^{-1/3} - \left(-\frac{z_t}{L_w} \right)^{-1/3} \right] \right\}, \\ T_z &= \frac{T_*}{\kappa} \left\{ \left[\ln \left(\frac{\zeta_h L_w}{z_{ot}} \right) - \psi_h(\zeta_h) \right] \right. \end{aligned} \quad (3.74)$$

$$\begin{aligned}
 & +0.8 \left[(-\zeta_h)^{-1/3} - \left(-\frac{z_t}{L_w} \right)^{-1/3} \right] \Big\} + T_0, \\
 T_* = T_z \kappa & \left\{ \left\{ \left[\ln \left(\frac{\zeta_h L_w}{z_{ot}} \right) - \psi_h(\zeta_h) \right] \right. \right. \\
 & \left. \left. +0.8 \left[(-\zeta_h)^{-1/3} - \left(-\frac{z_t}{L_w} \right)^{-1/3} \right] \right\} + T_0 \right\}^{-1}, \tag{3.75}
 \end{aligned}$$

$$\begin{aligned}
 T_{10} = \frac{T_*}{\kappa} & \left\{ \left[\ln \left(\frac{\zeta_h L_w}{z_{ot}} \right) - \psi_h(\zeta_h) \right] \right. \\
 & \left. +0.8 \left[(-\zeta_h)^{-1/3} - \left(-\frac{10}{L_w} \right)^{-1/3} \right] \right\} + T_0, \tag{3.76}
 \end{aligned}$$

for very unstable conditions ($\zeta < \zeta_h = -0.465$), where the stability function for temperature and humidity ($\psi_h = \psi_e$) is given by

$$\psi_h = \psi_e = 2 \ln \left(\frac{1 + \chi^2}{2} \right). \tag{3.77}$$

The calculation for q_* is the same as those for T_* except that $[T_z - T_0]$ and z_{ot} are replaced by $[q_z - q_0]$ and z_{oq} respectively:

$$\phi_e = \frac{\kappa z_q}{q_*} \frac{dq}{dz} = 5 + \zeta, \tag{3.78}$$

$$\phi_e = \frac{\kappa z_q}{q_*} \frac{dq}{dz} = 5 + \left(\frac{z_q}{L_w} \right),$$

and then by re-arranging for dq and integrating between z_{oq} and z_q we obtain

$$\begin{aligned}
 dq &= \frac{q_*}{\kappa} \left\{ \left[\ln \left(\frac{L_w}{z_{oq}} \right) + 5 \right] + \left[5 + \ln \left(\frac{z_q}{L_w} \right) + \left(\frac{z_q}{L_w} \right) - 1 \right] \right\}, \\
 q_z - q_0 &= \frac{q_*}{\kappa} \left\{ \left[\ln \left(\frac{L_w}{z_{oq}} \right) + 5 \right] + \left[5 + \ln \left(\frac{z_q}{L_w} \right) + \left(\frac{z_q}{L_w} \right) - 1 \right] \right\}, \\
 q_z &= \frac{q_*}{\kappa} \left\{ \left[\ln \left(\frac{L_w}{z_{oq}} \right) + 5 \right] + \left[5 + \ln \left(\frac{z_q}{L_w} \right) + \left(\frac{z_q}{L_w} \right) - 1 \right] \right\} + q_0,
 \end{aligned} \tag{3.79}$$

$$q_* = q_z \kappa \left\{ \left\{ \left[\ln \left(\frac{L_w}{z_{oq}} \right) + 5 \right] + \left[5 + \ln \left(\frac{z_q}{L_w} \right) + \left(\frac{z_q}{L_w} \right) - 1 \right] \right\} + q_0 \right\}^{-1}, \tag{3.80}$$

$$q_{10} = \frac{q_*}{\kappa} \left\{ \left[\ln \left(\frac{L_w}{z_{oq}} \right) + 5 \right] + \left[5 + \ln \left(\frac{10}{L_w} \right) + \left(\frac{10}{L_w} \right) - 1 \right] \right\} + q_0, \tag{3.81}$$

for very stable conditions ($\zeta > 1$),

$$\phi_e = \frac{\kappa z_q}{q_*} \frac{dq}{dz} = 1 + 5\zeta, \tag{3.82}$$

$$\phi_e = \frac{\kappa z_q}{q_*} \frac{dq}{dz} = 1 + 5 \left(\frac{z_q}{L_w} \right),$$

CHAPTER 3. BULK PARAMETERIZATION OF SURFACE FLUXES

and then by re-arranging for dq and integrating between z_{oq} and z_q we obtain

$$dq = \frac{q_*}{\kappa} \left[\ln \left(\frac{z_q}{z_{oq}} \right) + 5 \left(\frac{z_q}{L_w} \right) \right],$$

$$q_z - q_0 = \frac{q_*}{\kappa} \left[\ln \left(\frac{z_q}{z_{oq}} \right) + 5 \left(\frac{z_q}{L_w} \right) \right],$$

$$q_z = \frac{q_*}{\kappa} \left[\ln \left(\frac{z_q}{z_{oq}} \right) + 5 \left(\frac{z_q}{L_w} \right) \right] + q_0, \quad (3.83)$$

$$q_* = q_z \kappa \left\{ \left[\ln \left(\frac{z_q}{z_{oq}} \right) + 5 \left(\frac{z_q}{L_w} \right) \right] + q_0 \right\}^{-1}, \quad (3.84)$$

$$q_{10} = \frac{q_*}{\kappa} \left[\ln \left(\frac{10}{z_{oq}} \right) + 5 \left(\frac{10}{L_w} \right) \right] + q_0, \quad (3.85)$$

for stable conditions ($0 < \zeta < 1$),

$$\phi_e = \frac{\kappa z_q}{q_*} \frac{dq}{dz} = (1 - 16\zeta)^{-1/2}, \quad (3.86)$$

$$\phi_e = \frac{\kappa z_q}{q_*} \frac{dq}{dz} = \left(1 - 16 \left(\frac{z_q}{L_w} \right) \right)^{-1/2},$$

and then by re-arranging for dq and integrating between z_{oq} and z_q we obtain

$$dq = \frac{q_*}{\kappa} \left[\ln \left(\frac{z_q}{z_{oq}} \right) - \psi_e \left(\frac{z_q}{L_w} \right) \right],$$

$$q_z - q_0 = \frac{q_*}{\kappa} \left[\ln \left(\frac{z_q}{z_{oq}} \right) - \psi_e \left(\frac{z_q}{L_w} \right) \right],$$

$$q_z = \frac{q_*}{\kappa} \left[\ln \left(\frac{z_q}{z_{oq}} \right) - \psi_e \left(\frac{z_q}{L_w} \right) \right] + q_0, \quad (3.87)$$

$$q_* = q_z \kappa \left\{ \left[\ln \left(\frac{z_q}{z_{oq}} \right) - \psi_e \left(\frac{z_q}{L_w} \right) \right] + q_0 \right\}^{-1}, \quad (3.88)$$

$$q_{10} = \frac{q_*}{\kappa} \left[\ln \left(\frac{10}{z_{oq}} \right) - \psi_e \left(\frac{10}{L_w} \right) \right] + q_0, \quad (3.89)$$

for unstable conditions ($\zeta_e < \zeta < 0$), and

$$\phi_e = \frac{\kappa z_q}{q_*} \frac{dq}{dz} = 0.9 \kappa^{4/3} (-\zeta)^{-1/3}, \quad (3.90)$$

$$\phi_e = \frac{\kappa z_q}{q_*} \frac{dq}{dz} = 0.9 \kappa^{4/3} \left(-\frac{z_q}{L_w} \right)^{-1/3}, \quad (3.91)$$

and then by re-arranging for dq and integrating between z_{oq} and z_q we obtain

$$\begin{aligned} dq &= \frac{q_*}{\kappa} \left\{ \left[\ln \left(\frac{\zeta_e L_w}{z_{oq}} \right) - \psi_e(\zeta_e) \right] \right. \\ &\quad \left. + 0.8 \left[(-\zeta_e)^{-1/3} - \left(-\frac{z_q}{L_w} \right)^{-1/3} \right] \right\}, \\ q_z - q_0 &= \frac{q_*}{\kappa} \left\{ \left[\ln \left(\frac{\zeta_e L_w}{z_{oq}} \right) - \psi_e(\zeta_e) \right] \right. \\ &\quad \left. + 0.8 \left[(-\zeta_e)^{-1/3} - \left(-\frac{z_q}{L_w} \right)^{-1/3} \right] \right\}, \\ q_z &= \frac{q_*}{\kappa} \left\{ \left[\ln \left(\frac{\zeta_e L_w}{z_{oq}} \right) - \psi_e(\zeta_e) \right] \right. \end{aligned} \quad (3.92)$$

$$\begin{aligned}
 & +0.8 \left[(-\zeta_e)^{-1/3} - \left(-\frac{z_q}{L_w} \right)^{-1/3} \right] \Bigg\} + q_0, \\
 q_* = q_z \kappa & \left\{ \left\{ \left[\ln \left(\frac{\zeta_e L_w}{z_{oq}} \right) - \psi_e(\zeta_e) \right] \right. \right. \\
 & \left. \left. +0.8 \left[(-\zeta_e)^{-1/3} - \left(-\frac{z_q}{L_w} \right)^{-1/3} \right] \right\} + q_0 \right\}^{-1}, \tag{3.93}
 \end{aligned}$$

$$\begin{aligned}
 q_{10} = \frac{q_*}{\kappa} & \left\{ \left[\ln \left(\frac{\zeta_e L_w}{z_{oq}} \right) - \psi_e(\zeta_e) \right] \right. \\
 & \left. +0.8 \left[(-\zeta_e)^{-1/3} - \left(-\frac{10}{L_w} \right)^{-1/3} \right] \right\} + q_0, \tag{3.94}
 \end{aligned}$$

for very unstable conditions ($\zeta < \zeta_e = -0.465$).

The transfer coefficients for momentum (C_{dz}), sensible heat (C_{hz}) and latent heat (C_{ez}) at the measurement height can be calculated by re-arranging equations 3.23 to 3.25 as:

$$\tau = C_{dz} \rho_z u_z^2 = \rho_z u_{*a}^2, \tag{3.95}$$

$$C_{dz} = \rho_z u_{*a}^2 / \rho_z u_z^2, \tag{3.96}$$

$$C_{dz} = u_{*a}^2 / u_z^2, \tag{3.97}$$

$$Q_h = \rho_z C_{pa} C_{hz} u_z (T_0 - T_z) = \rho_z C_{pa} u_{*a} T_*, \tag{3.98}$$

$$C_{hz} = \rho_z C_{pa} u_{*a} T_* / \rho_z C_{pa} u_z (T_0 - T_z), \tag{3.99}$$

$$C_{hz} = -u_{*a} T_* / u_z (T_0 - T_z). \tag{3.100}$$

$$Q_e = \rho_z L_v C_{ez} u_z (q_0 - q_z) = -\rho_z L_v u_{*a} q_*, \tag{3.101}$$

$$C_{ez} = \rho_z L_v u_z (q_0 - q_z) \Big/ -\rho_z L_v u_{*a} q_*, \quad (3.102)$$

$$C_{ez} = -u_{*a} q_* \Big/ u_z (q_0 - q_z). \quad (3.103)$$

In order to compare the transfer coefficients among sites we also need to calculate them at a reference height of 10 m ($C_{d10}, C_{h10}, C_{e10}$) as:

$$C_{h10} = Q_h \Big/ \rho_z C_{pa} u_{10} (T_0 - T_{10}), \quad (3.104)$$

$$C_{e10} = Q_e \Big/ \rho_z L_v u_{10} (q_0 - q_{10}), \quad (3.105)$$

$$C_{d10} = u_{*a}^2 \Big/ u_{10}^2. \quad (3.106)$$

We can also calculate the neutral transfer coefficient at a height of 10 m as:

$$C_{d10N} = \left[\kappa \Big/ \ln \left(\frac{10}{z_o} \right) \right]^2, \quad (3.107)$$

$$C_{e10N} = C_{h10N} = \kappa^2 \Big/ \left[\ln \left(\frac{10}{z_o} \right) \ln \left(\frac{10}{z_{oq}} \right) \right], \quad (3.108)$$

where z_o and z_{oq} are calculated under neutral atmospheric conditions, that is $\zeta = 0$.

3.4 Evaporation

Evaporation is a key component in the water and energy budgets of lakes, where in most cases, represents major water loss. Information on lake evaporation, is therefore, essential for water resource management and for predicting future changes in water levels as a result of climate change. Here, evaporation (E) is estimated according to the latent heat flux (Q_e) as

$$E = \frac{Q_e}{\rho_0 \times L_v}, \quad (3.109)$$

where ρ_0 is the density of the surface water.

References

- Atwater, M. A. and Brown, P. S., 1974, Numerical computations of the latitudinal variation of solar radiation for an atmosphere of varying opacity, *Journal of Applied Meteorology* **13**, 289–297.
- Bolton, D., 1980, The computation of equivalent potential temperature, *Monthly Weather Review* **108**, 1046–1053.
- Brutsaert, W., 1982, *Evaporation Into the Atmosphere: Theory, History and Applications*, Environmental Fluid Mechanics, Springer.
- Crawford, T. and Duchon, C., 1999, An improved parameterization for estimating effective atmospheric emissivity for use in calculating daytime downwelling longwave radiation, *Journal of Applied Meteorology* **38**, 474–480.
- Davies, J. A., Robinson, P. J. and Nunez, M., 1971, Field determinations of surface emissivity and temperature for Lake Ontario, *Journal of Applied Meteorology* **10**(4), 811–819.

REFERENCES

- Fairall, C., Bradley, E., Hare, J., Grachev, A. and Edson, J., 2003, Bulk parameterization of air-sea fluxes: updates and verification for the coare algorithm, *Journal of Climate* **16**, 571–591.
- Fairall, C. W., Bradley, E. F., Rogers, D. P., Edson, J. B. and Young, G. S., 1996, Bulk parameterization of air-sea fluxes for Tropical Ocean-Global Atmosphere Coupled-Ocean Atmosphere Response Experiment, *Journal of Geophysical Research Oceans* **101**, 3747–3764. doi: 10.1029/95JCO3205.
- Gill, A. E., 1982, *Atmosphere-Ocean dynamics*, International Geophysics, Elsevier Science.
- Houghton, H. G., 1954, On the annual heat balance of the northern hemisphere, *Journal of Meteorology* **11**(1), 1–9.
- Jakkila, J., Lepparanta, M., Kawamura, T., Shirasawa, K. and Salonen, K., 2009, Radiation transfer and heat budget during the ice season in Lake Pääjärvi, Finland, *Aquatic Ecology* **43**(3), 681–692.
- Kirk, J. T. O., 1994, *Light and photosynthesis in aquatic ecosystems*, Cambridge University Press.
- Kondratyev, K., 1969, *Radiation in the atmosphere*, International Geophysics, Elsevier Science.
- Lowe, P. R., 1977, An approximating polynomial for the computation of saturation vapor pressure, *Journal of Applied Meteorology* **16**, 100–103.

- McDonald, J. E., 1960, Direct absorption of solar radiation by atmospheric water vapor, *Journal of Meteorology* **17**(3), 319–328.
- Meyers, T. P. and Dale, R. F., 1983, Predicting daily insolation with hourly cloud height and coverage, *Journal of Climate and Applied Meteorology* **22**(4), 537–545.
- Monin, A. and Obukhov, A., 1954, Basic laws of turbulent mixing in the atmosphere near the ground, *J. Akad. Nauk. SSR Geofiz. Inst* **64**, 1963–1987.
- Read, J., Hamilton, D., Jones, I., Muraoka, K., Winslow, L., Kroiss, R., Wu, C. and Gaiser, E., 2011, Derivation of lake mixing and stratification indices from high-resolution lake buoy data, *Environmental Modelling and Software* **26**(11), 1325 – 1336.
- Read, J. S., Hamilton, D. P., Desai, A. R., Rose, K. C., MacIntyre, S., Lenters, J. D., Smyth, R. L., Hanson, P. C., Cole, J. J., Staehr, P. A., Rusak, J. A., Pierson, D. C., Brookes, J. D., Laas, A. and Wu, C. H., 2012, Lake-size dependency of wind shear and convection as controls on gas exchange, *Geophysical Research Letters* **39**(9). doi: 10.1029/2012GL051886.
- Smith, S., 1998, Coefficients for sea surface wind stress, heat flux, and wind profiles as a function of wind speed and temperature, *Journal of Geophysical Research* **93**, 15467–15472. doi: 10.1029/JC093iC12p15467.

REFERENCES

- Smith, W. L., 1966, Note on the relationship between total precipitable water and surface dewpoint, *Journal of Applied Meteorology* **5**, 726–727.
- Verburg, P. and Antenucci, J., 2010, Persistent unstable atmospheric boundary layer enhances sensible and latent heat loss in a tropical great lake: Lake Tanganyika, *Geophysical Research Letters* **115**.
- Zeng, X., Zhao, M. and Dickinson, R., 1998, Intercomparison of bulk aerodynamic algorithms for the computation of sea surface fluxes using togo coare and tao data, *Journal of Climate* **11**, 2628:2644.